

Kinetic Study and Modelling of n-Heptane Reforming Process over Pt/Zr-HMS/HZSM-5 Composite Catalysts

M.H. Peyrovi^{a,*}, N. Parsafard^{b,*} and A. Sajedi^a

^a*Faculty of Chemistry Science and Petroleum, Department of Physical Chemistry, University of Shahid Beheshti, Tehran, 1983963113, Iran*

^b*Kosar University of Bojnord, Department of Applied Chemistry, North Khorasan, Iran*

(Received 9 August 2018, Accepted 21 October 2018)

Pt/Zr(x)-HMS/HZSM-5 catalysts with various Si/Zr ratios (as x) were used for investigation of the kinetics of n-heptane reforming process under 350-450 °C reaction temperature, 35-80 ml min⁻¹ flowing rate of hydrogen and 2-5 ml h⁻¹ flowing rate of n-heptane. In the present work, two kinetic models, power law and Langmuir-Hinshelwood, were selected and examined to describe the kinetics of the n-heptane reforming process over the used catalysts. The results show that the Langmuir-Hinshelwood model provides a better fit with the experimental data and allows to determine the kinetic parameters. Among the synthesized catalysts, Pt/Zr(35)-HMS/HZSM-5 (with Si/Zr = 35) has the best performance for this process, because this catalyst, in contrast to others, based on the apparent activation energies, has a quick formation of aromatic and isomeric products, and low rate on the production of by-products, such as cracking and hydrogenolysis products.

Keywords: Reforming, Kinetics, Power law model, Langmuir-Hinshelwood model

INTRODUCTION

The catalytic reforming of hydrocarbons is an important process within the petroleum refining industry for production of aromatic compounds and gasoline with a high octane number [1]. Generally, the heavy straight run gasoline (HSRG), including paraffins, olefins, naphthenes and aromatics (PONA) with 5 to 10 carbon atoms are used as a feed for this process [2]. High-yield for converting light straight-run naphtha into aromatics is very important for promoting the octane number of gasoline. Accordingly, the aromatization of n-heptane is a significant reaction of reforming, especially on platinum supported catalysts [3]. However, the current environmental regulations control the total amounts of aromatic compounds in gasoline, particularly benzene, due to their toxic and carcinogenic

properties. Some of the other desirable reactions causing the increase in the octane number are isomerization and cyclization, which can be suitable substitute reactions for aromatization [4,5].

Many researchers have focused on the activity, products distribution and selective behavior of various catalysts in this process [4-6]. However, relatively few studies have been published on the kinetics of hydrocarbons reforming [7]. This might be due to a significant number of reactions occurring during this process [3]. On this basis, a detailed kinetic study considering all components and reactions occurred in the reforming of hydrocarbons is too complex and difficult. To decrease these complications, the components in the produced mixture are divided into some limited groups. In this respect, the most important reactions in this process have been classified under four groups, namely, isomerization to isoparaffins, cracking of paraffins to lower hydrocarbons, aromatization and hydrogenolysis [8]. Many attempts have been made to develop the kinetics

*Corresponding authors. E-mail: m-peyrovi@sbu.ac.ir;
n-parsafard@kub.ac.ir

of catalytic reforming with an efficient catalyst [9]. In this work, the kinetics of n-heptane reforming are investigated over a series of Pt/Zr(x)-HZSM-5/HMS catalysts with different Si/Zr ratios. The purpose of the present research is to find a suitable kinetic model under various operating conditions that represents the agreement between the estimated data and experimental results obtained from the novel bifunctional catalysts in the n-heptane reforming.

EXPERIMENTAL

A series of Zr(x)-HMS/HZSM-5 catalysts with 40 wt% of H-ZSM-5 and various molar ratios of Si/Zr were synthesized according to our previous work procedure [10]. Briefly, the precursors of Zr-HMS include zirconyl (IV) nitrate hydrate, tetra ethyl ortho silicate, ethanol, dodecyl amine, HCl 1 M, HNO₃ 0.01 M with the prepared H-ZSM-5 were dissolved in deionized water, step by step, and stirred separately for a certain period of time. The as-prepared precipitate was aged for 20 h, dried overnight at room temperature and calcined at 600 °C for 6 h under air flow. These denoted supports, Zr(x)-HZ, were impregnated by a concentration of H₂PtCl₆ solution for preparing the Pt (0.6 wt%) supported catalysts. Then, the obtained material was dried at 110 °C and calcined in air at 300 °C for 4 h. The Pt supported Zr(x)-HMS/HZSM-5 catalysts were named Pt/Zr(x)-HZ that x represents the nominal Si/Zr ratios equal to 5, 10, 20 and 35.

1 g of each catalyst was investigated for kinetic study in a continuous fixed-bed Pyrex microreactor operated under isothermal conditions and connected to an on-line gas chromatograph (Agilent Technologies 7890A equipped with a flame ionization detector) by a controller. Each catalyst was heated and reduced in 40 ml min⁻¹ H₂ at 450 °C for 2 h. Then, these samples were cooled until the reaction temperature. At this step, the reaction was started by switching feed from hydrogen to a mixture of n-heptane and hydrogen.

In this kinetic study, two sets of experimental conditions were examined under the following conditions. 2-5 ml h⁻¹ flow rate of n-C₇ and 40 ml min⁻¹ flow rate of H₂, and 35-80 ml min⁻¹ flow rates of H₂ and 2 ml h⁻¹ flow rate of n-C₇. These flow rates were yielded for a residence time of 1 h at each temperature within the range of 350-450 °C. All rate

measurements at different temperatures, and reactant pressures were also done at 1 h of reaction. The reaction products were analyzed by gas chromatography and a flame ionization detector.

In the present work, the main reactions of the n-C₇ reforming were considered. This process was divided into four important reactions as isomerization (i-C₇), cracking (crack.), aromatization (arom.) and hydrogenolysis (hydro.). On this basis, the kinetics calculations will be performed in accordance with this division. Two kinetics models were used to simulate the kinetics of mentioned reactions. The partial orders of these reactions and other kinetic parameters were calculated based on the simplest model (power law model).

Power Law (PL) Model

Power law model was chosen for simulating the reaction kinetics as an easiest model available. The kinetic expression as a function of n-C₇ and H₂ pressures is as follows;

$$r\left(\frac{\text{mol}}{\text{g s}}\right) = kP_{\text{H}_2}^n P_{\text{C}_7}^m \quad (1)$$

where r is the rate of each reaction (mol g⁻¹ s⁻¹); k is the rate constant; P_{H₂} is the partial pressure of H₂ (P_a); P_{C₇} is the partial pressure of n-C₇ (P_a), and n and m are the rate exponents for each reaction [11,12].

The rate constant (k) also was measured using the Arrhenius equation;

$$k = Ae^{-\frac{E_{app}^{act}}{RT}} \quad (2)$$

where E_{app}^{act} is the apparent activation energy (kJ mol⁻¹); R, the gas constant (kJ mol⁻¹ K⁻¹); A, the pre-exponential factor, and T, the reaction temperature (K).

The reaction rates were measured under low conversion conditions (<10%) for producing a linear Arrhenius plot. The adjustment method includes to solve Eqs. (1) and (2) using the obtained experimental data.

For calculating the rate of each reaction and catalyst, the following equation was used for these measurements as a formula of reaction rate.

$$r \left(\frac{\text{mol}}{\text{g s}} \right) = \frac{n - C_7 \text{ flow rate} \times n - C_7 \text{ density} \times \text{conv.}(\%)}{n - C_7 \text{ molar weight} \times \text{weight of catalyst} \times \text{impregnated metal}} \quad (3)$$

Based on this model, to measure the n-C₇ exponent (m), the prepared catalysts were tested at 350-450 °C for a series of various gaseous feed with n-C₇ flow rates over the range of 2-5 ml h⁻¹, whereas the H₂ flow rate at 40 ml min⁻¹ was maintained constant. After each reaction, the used catalysts were cleaned under H₂ flow while heating them at 450 °C before cooling to 350 °C and continuing the other step of reaction. Similarly, the H₂ exponent (n) was measured through this procedure. So, the flow rate of H₂ was varied between 35 and 80 ml min⁻¹ while maintaining the n-C₇ at 2 ml h⁻¹ flow rate. After each experiment, the obtained products were analyzed using the on-line gas chromatography at a fixed interval of time (1 h). Other kinetic parameters in these equations were estimated by the experimental data measured from these kinetic tests.

Langmuir Model

There are two proposed mechanisms through this model, the Eley-Rideal (ER) and the Langmuir-Hinshelwood (LH) mechanisms. According to the vast majority of the reported surface catalytic reactions, it has been accepted that the occurrence of these reactions between two adsorbed molecules (Langmuir-Hinshelwood mechanism) [13] is preferred. The kinetic expression of this mechanism for the gas phase can be expressed as follows;

$$r = \frac{k P_{C_7} P_{H_2}}{\left(\frac{1}{k_{C_7}} + P_{C_7} \right) \left(\frac{1}{k_{H_2}} + P_{H_2} \right)} \quad (4)$$

where k is the rate constant, and k_{H₂} and k_{C₇} are the adsorption constants of H₂ and n-C₇. In this equation, it was assumed that the adsorption constants (k_{H₂} and k_{C₇}) correspond to a van't Hoff type equation [13].

$$k_x = A_x e^{-\frac{\Delta H_{ads-x}}{RT}} \quad (5)$$

Equations (2) and Eq. (5) can expand the expression of Eq. (4).

$$r = \frac{Ae^{-\frac{E_{app}}{RT}} P_{C_7} P_{H_2}}{\left(\frac{1}{A_{C_7} e^{-\frac{\Delta H_{ads-C_7}}{RT}} + P_{C_7}} \right) \left(\frac{1}{A_{H_2} e^{-\frac{\Delta H_{ads-H_2}}{RT}} + P_{H_2}} \right)} \quad (6)$$

Consequently, the pre-exponential factors, activation energies and heats of adsorption can be estimated by a numerical method. The kinetic parameters of these models were estimated by numerical integrations to obtain the best fit between the experimental data and the calculated rate equation.

RESULTS AND DISCUSSIONS

To confirm the absence of external diffusion limitations and their effects upon the results of the catalytic performances, several experiments were conducted under an external diffusion regime. On this basis, five different amounts of each catalyst were selected within the range of 0.5-1.5 g. The results show that in the weights over 1.0 g of catalysts, the reaction is affected by an external diffusion. To avoid this effect, a catalyst bed containing 1.0 g of catalyst or lower amount was employed. The internal diffusion limitations were also investigated by changing the average particle size in three ranges of 50-150, 150-250 and 250-350 μm. The results of reaction rates at various temperatures showed that the catalysts with the smallest particles size (50-150 μm) have no internal diffusion limitation. As a result, this catalytic study was carried out with the particle size in the range of 50-150 μm.

In order to recognize the mechanism of n-C₇ reforming process over the prepared catalysts, the fit of two kinetic models with obtained experimental results was evaluated and discussed independently.

Power Law (PL) Model

The apparent activation energies (E_{app}^{act}) for each catalyst were calculated by the logarithmic form for the Arrhenius equation (Eq. (2)). The plots of lnK vs. 1/T calculated from the experimental data over different prepared catalysts in the isomerization reaction (one selected reaction of n-C₇ reforming reactions) have been presented in Fig. 1.

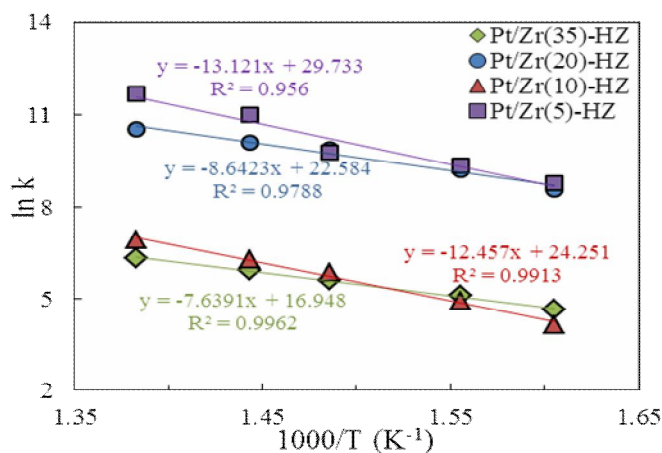


Fig. 1. Arrhenius plots obtained from the experimental data.

The apparent activation energies measured at 350-450 °C for all reactions in the gas phase of n-C₇ reforming are summarized in Table 1. The correlation coefficients (R²) of these plots (Arrhenius plots) were obtained above 0.95 showing a good fit to the experimental data. From the slope of these plots, the apparent activation energies were approximated to be in the ranges of 64.1-107.1 (for isomerization reaction), 157.9-271.2 (for cracking reaction), 37.6-48.3 (for hydrogenolysis reaction) and 109.4-129.5 (for aromatization reaction) kJ mol⁻¹. These results indicate that among four main reactions occurred during this process, the cracking reaction performs hardly because of its higher activation energies. As a result, less cracking products are produced from the synthesized catalysts, which is a very desirable deficit. While the hydrogenolysis reaction is the fastest and easiest response based on the activation energies, the reaction such as cracking is not desired and should be minimized. According to the activation energies of isomerization reaction, this reaction has also the good conditions for performing. These data are very sparse, such as the activation energies reported in the literature [3,8] for the gas-phase reforming of n-C₇ over the supported catalysts.

The observed reaction rates as a function of the partial pressures of each reactant in the logarithm form are shown in Fig. 2. In this figure, the partial pressures of n-C₇ (or H₂) were changed while the other component pressure was kept constant [14].

This figure shows that the reaction rate increases with

increasing the pressure of n-C₇, whereas the reaction rate decreases slightly with increasing the pressure of H₂. Three parameters of the PL model (k, m and n) based on Eq. (1) were measured by multiple regression analysis at different temperatures. The results of estimated i-C₇ selectivity versus experimental data (just isomerization reaction is shown here) are presented in Fig. 3. The fitness of the PL model to the experimental data is evidenced by the slope of unity and correlation coefficient. The calculated data with this model present a good fitness with the experimental data (R² = 0.99). Although the PL model is a mathematic model and does not have a direct connection with the reaction mechanism [15], the estimated kinetic results from this model are similar to those reported in literature [15,16] for this reaction. Accordingly, it seems that this model is approximately sufficient to represent the kinetic behavior and parameters obtained from the prepared catalysts for the reactions of n-C₇ reforming.

The measured values of n and m from this model show the negative values for hydrogen in the isomerization, cracking and hydrogenolysis reactions. The negative rate exponents of hydrogen in these reactions show the inhibitory effect of this compound, and the positive exponents show the strong adsorption on the catalysts surfaces.

Langmuir-Hinshelwood (LH) Model

Same experiments as PL model were done in this section. Kinetic parameters of Eq. (6) have been estimated

Table 1. H₂ and n-C₇ Exponents and Activation Energies Estimated by the Power Law Model for Various Reactions of n-C₇ Reforming

Catalysts	Orders	T (°C)	i-C ₇	Crack.	Hydro.	Arom.
	n _{H2}	350	-0.5	-1.2	-1.1	1.1
		400	-0.3	-0.5	-0.7	0.7
		450	-0.2	-0.2	-0.4	0.6
Pt/Zr(5)-HZ	m _{C7}	350	1.4	1.3	1.6	0.8
		400	1.2	1.0	1.2	0.4
		450	1.0	0.9	1.1	0.2
	E_{app}^{act} (kJ mol ⁻¹)		107.1	157.9	37.6	129.5
	n _{H2}	350	-0.7	-1.2	-0.7	1.1
		400	-0.3	-0.5	-0.4	0.6
		450	-0.2	-0.3	-0.4	0.6
Pt/Zr(10)-HZ	m _{C7}	350	1.1	1.9	1.4	0.7
		400	0.9	1.2	1.1	0.3
		450	0.9	1.0	1.1	0.2
	E_{app}^{act} (kJ mol ⁻¹)		104.5	158.0	38.5	126.3
	n _{H2}	350	-0.3	-1.0	-1.0	0.8
		400	-0.2	-0.4	-0.5	0.6
		450	-0.2	-0.3	-0.4	0.5
Pt/Zr(20)-HZ	m _{C7}	350	1.3	1.8	1.3	0.4
		400	1.1	1.1	1.1	0.2
		450	1.0	1.0	1.0	0.1
	E_{app}^{act} (kJ mol ⁻¹)		73.7	187.4	48.3	119.9
	n _{H2}	350	-0.5	-0.8	-0.5	1.2
		400	-0.3	-0.3	-0.3	0.6
		450	-0.2	-0.2	-0.2	0.6
Pt/Zr(35)-HZ	m _{C7}	350	1.0	1.9	1.6	0.9
		400	0.9	1.1	1.2	0.3
		450	0.9	1.0	1.1	0.2
	E_{app}^{act} (kJ mol ⁻¹)		64.1	271.2	61.2	109.4

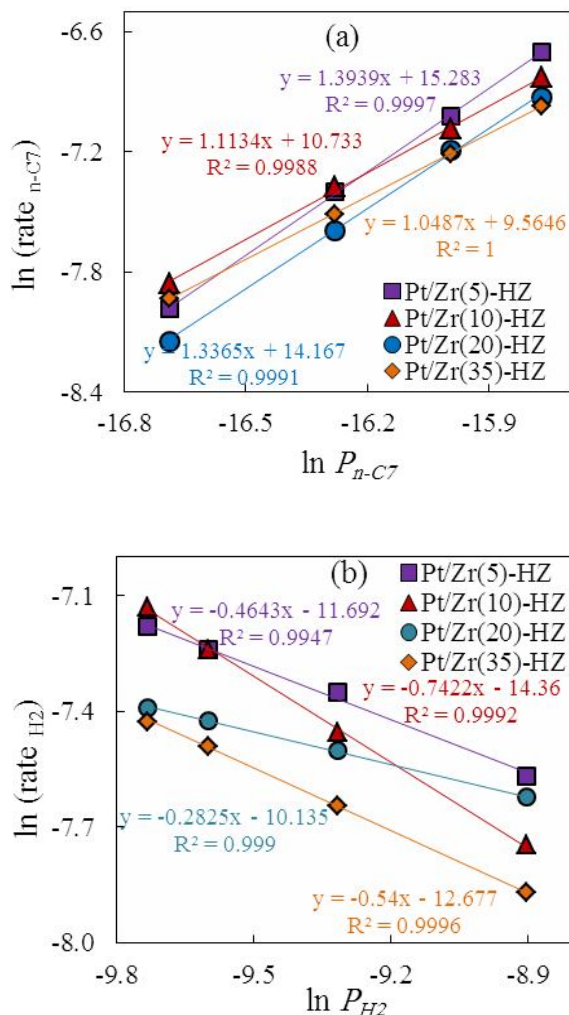


Fig. 2. Double-log plots of the reaction rates versus the partial pressures of (a) n-C₇ and (b) H₂.

for each reaction mentioned in the n-C₇ reforming process. These data are listed in Table 2. These results show that the activation energies calculated via the LH model vary with the activation energies measured by the PL model. This observation is probably because the molecular adsorption and interaction have not been considered by this model because of its mathematical nature. The negative values of the adsorption heats for the n-C₇ ($\Delta H_{\text{ads-C}_7}$) and H₂ ($\Delta H_{\text{ads-C}_7}$) in Table 2 show the exothermic natures of these adsorptions in the reforming process.

Table 2 summarizes the pre-exponential factors of H₂ (A_{H_2}) and n-C₇ (A_{C_7}) adsorptions. This factor for n-C₇ is almost the same for all catalysts, and for hydrogen is small

in most cases. The smaller pre-exponential factor probably implies a slower and weaker adsorption for respective component over the surfaces of catalysts. These results are in full compliance with the activity and selectivity of catalysts.

The parameters obtained were used to simulate the selectivity of catalysts to various products. The results of simulated i-C₇ selectivity by LH models to experimental data are presented in Fig. 4.

The results show that the calculated data concerning the LH model present a same trend to the experimental results, and the accuracy of these data ($R^2 \sim 1.00$) is better than the simulated results with PL model.

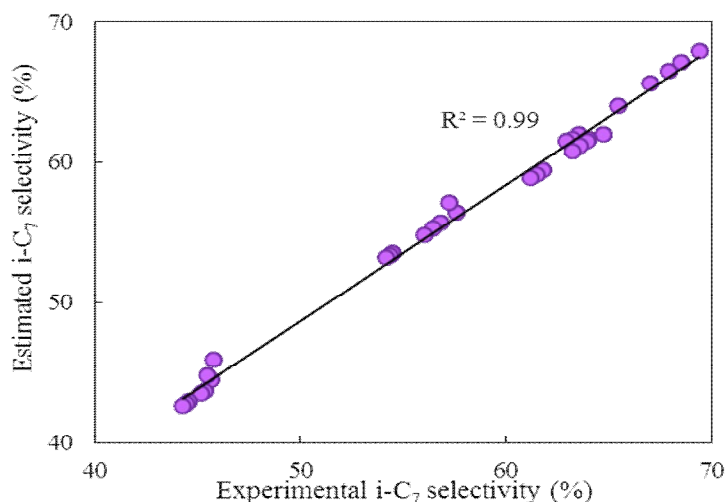


Fig. 3. Estimated data by power law model. These plots are presented only for one of the selected reactions (isomerization) in the n-C₇ reforming.

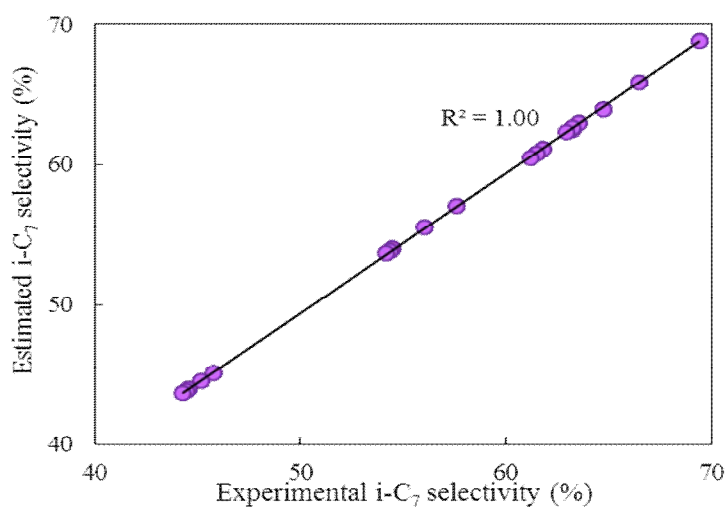


Fig. 4. Estimated data by Langmuir-Hinshelwood model. These plots are presented only for one of the selected reactions (isomerization) in the n-C₇ reforming.

CONCLUSIONS

The kinetics of n-C₇ reforming over a series of Pt based catalysts has been examined as a function of n-C₇ and H₂ partial pressures at various temperatures. The reaction orders of hydrogen are negative with respect to isomerization, cracking and hydrogenolysis reactions,

suggesting the inhibiting effect of H₂ and positive with respect to n-C₇, indicating the strong coverage of catalysts by n-C₇. The kinetic tests show that these catalysts (especially Pt/Zr(35)-HZ) perform the n-C₇ reforming process with a proper rate. The activation energies calculated in this work confirm that these catalysts are attractive supports for this process. Furthermore, two kinetic

Table 2. Kinetic Parameters and Activation Energies Estimated by Langmuir-Hinshelwood Model for Various Reactions of n1-C₇ Reforming

Catalysts		Parameters	i-C ₇	Crack.	Hydro.	Arom.	
Pt/Zr(5)-HZ	K	E_{app}^{act} (kJ mol ⁻¹)	121.6	70.8	9.6	182.8	
		A (mol g ⁻¹ s ⁻¹)	1.2×10^{-7}	1.4×10^{-12}	1.7×10^{-16}	1.4×10^{-4}	
	K _{C7}	$-\Delta H_{ada-C7}$ (kJ mol ⁻¹)	5.6	5.6	5.6	5.6	
		A _{C7} (atm ⁻¹)	20.2	20.2	20.2	20.2	
	K _{H2}	$-\Delta H_{ada-H2}$ (kJ mol ⁻¹)	98.6	112.6	63.9	46.9	
		A _{H2} (atm ⁻¹)	2.0×10^{-9}	1.9×10^{-27}	1.6×10^{-21}	9.3×10^{-22}	
	Pt/Zr(10)-HZ	K	E_{app}^{act} (kJ mol ⁻¹)	119.4	103.4	41.5	166.4
			A (mol g ⁻¹ s ⁻¹)	2.6×10^{-8}	9.0×10^{-11}	1.4×10^{-14}	1.6×10^{-4}
K _{C7}		$-\Delta H_{ada-C7}$ (kJ mol ⁻¹)	5.6	5.6	5.6	5.6	
		A _{C7} (atm ⁻¹)	20.2	20.2	20.2	20.2	
K _{H2}		$-\Delta H_{ada-H2}$ (kJ mol ⁻¹)	72.5	94.8	93.0	102.8	
		A _{H2} (atm ⁻¹)	1.3×10^{-11}	6.0×10^{-26}	8.5×10^{-26}	1.3×10^{-26}	
Pt/Zr(20)-HZ		K	E_{app}^{act} (kJ mol ⁻¹)	117.1	134.2	58.8	138.8
			A (mol g ⁻¹ s ⁻¹)	8.6×10^{-9}	4.3×10^{-8}	1.5×10^{-12}	7.9×10^{-8}
	K _{C7}	$-\Delta H_{ada-C7}$ (kJ mol ⁻¹)	5.6	5.6	5.6	5.6	
		A _{C7} (atm ⁻¹)	20.2	20.2	20.2	20.2	
	K _{H2}	$-\Delta H_{ada-H2}$ (kJ mol ⁻¹)	68.8	37.9	35.4	99.8	
		A _{H2} (atm ⁻¹)	4.7×10^{-12}	5.5×10^{-19}	1.4×10^{-20}	9.3×10^{-10}	
	Pt/Zr(35)-HZ	K	E_{app}^{act} (kJ mol ⁻¹)	116.4	149.2	104.3	97.8
			A (mol g ⁻¹ s ⁻¹)	5.2×10^{-9}	1.3×10^{-6}	9.6×10^{-10}	5.0×10^{-11}
K _{C7}		$-\Delta H_{ada-C7}$ (kJ mol ⁻¹)	5.6	6.3	5.6	5.8	
		A _{C7} (atm ⁻¹)	20.2	23.0	20.2	21.3	
K _{H2}		$-\Delta H_{ada-H2}$ (kJ mol ⁻¹)	98.0	196.3	140.8	112.0	
		A _{H2} (atm ⁻¹)	4.7×10^{-10}	1.4×10^{-33}	4.2×10^{-7}	11.8×10^5	

models (power law and Langmuir-Hinshelwood) were tested by first estimating kinetic parameters, and then estimated selectivity data were compared to experimental

data to validate the model. This modeling study indicates that the reactions of this process are good described by the Langmuir-Hinshelwood model, suggesting the reaction

mechanism.

REFERENCES

- [1] Vicerich, M. A.; Especel, C.; Benitez, V. M.; Epron, F.; Pieck, C. L., Influence of gallium on the properties of Pt-Re/Al₂O₃ naphtha reforming catalysts, *Appl. Catal. A: Gen.* **2011**, *407*, 49-55, DOI: 10.1016/j.apcata.2011.08.022.
- [2] Mohaddecy, R. S.; Sadighi, S., Developing a steady-state kinetic model for industrial scale semi-regenerative catalytic naphtha reforming process, *Chem. Ind.* **2014**, *63*, 149-154, DOI: 10.15255/KUI.2013.009.
- [3] Olafadehan, O. A.; Susu, A. A.; Jaiyeola, A., Mechanistic kinetic models for n-heptane reforming on platinum/alumina catalyst, *Petrol. Sci. Technol.* **2008**, *26*, 1459-1480, DOI: 10.1080/10916460701675157.
- [4] Peyrovi, M. H.; Parsafard, N.; Peyrovi, P., Influence of zirconium addition in platinum-hexagonal mesoporous silica (Pt-HMS) catalysts for reforming of n-heptane, *Ind. Eng. Chem. Res.* **2014**, *53*, 14253-14262, DOI: 10.1021/ie5024244.
- [5] Babaqi, B. S.; Takriff, M. S.; Kamarudin, S. K.; Othman, N. T. A.; Ba-Abbad, M. M., Comparison of catalytic reforming processes for process integration opportunities: *Brief Review, Int. J. Appl. Eng. Res.* **2016**, *11*, 9984-9989.
- [6] Yeh, Y. H.; Zhu, S.; Staiber, P.; Lobo, R. F.; Gorte, R. J., Zn-promoted H-ZSM-5 for endothermic Reforming of n-hexane at high pressures, *Ind. Eng. Chem. Res.* **2016**, *55*, 3930-3938, DOI: 10.1021/acs.iecr.6b00639.
- [7] Elizalde, I.; Ancheyta, J., Dynamic modeling and simulation of a naphtha catalytic reforming reactor, *Appl. Math. Model.* **2015**, *39*, 764-775, DOI: 10.1016/j.apm.2014.07.013.
- [8] Ancheyta-Juarez, J.; Villafuerte-Macias, E., Kinetic modeling of naphtha catalytic reforming reactions, *Energy Fuel.* **2000**, *14*, 1032-1037, DOI: 10.1021/ef0000274.
- [9] Stijepovic, M. Z.; Vojvodic-Ostojic, A.; Milenkovic, I.; Linke, P., Development of a kinetic model for catalytic reforming of naphtha and parameter estimation using industrial plant data, *Energy Fuel.* **2009**, *23*, 979-983, DOI: 10.1021/ef800771x.
- [10] Parsafard, N.; Peyrovi, M. H.; Jarayedi, M., Catalytic study and kinetic modeling of the n-heptane isomerization over Pt/Al-HMS/HZSM-5 hybrid catalysts, *Energy Fuel.* **2017**, *31*, 6389-6396, DOI: 10.1021/acs.energyfuels.7b00657.
- [11] Parsafard, N.; Peyrovi, M. H.; Rashidzadeh, M., Experimental and kinetic study of n-heptane isomerization on nanoporous Pt-(Re,Sn)/HZSM5-HMS catalysts, *Chin. J. Catal.* **2016**, *37*, 1477-1486, DOI: 10.1016/S1872-2067(15)61114-7.
- [12] Parsafard, N.; Peyrovi, M. H.; Parsafard, N., Effect of WO_x promoter on Pt/ZrO₂-HMS catalysts for n-heptane isomerization: Catalytic performance and kinetics study, *Chin. Chem. Lett.* **2017**, *28*, 546-552, DOI: 10.1016/j.ccl.2016.10.028.
- [13] Everaert, K.; Baeyens, J., Catalytic combustion of volatile organic compounds, *J. Hazard. Mat.* **2004**, *109*, 113-139, DOI: 10.1016/j.jhazmat.2004.03.019.
- [14] Kim, H. Y.; Lee, H. M.; Park, J. N., Bifunctional mechanism of CO₂ methanation on Pd-MgO/SiO₂ catalyst: Independent roles of MgO and Pd on CO₂ methanation, *J. Phys. Chem. C* **2010**, *114*, 7128-7131, DOI: 10.1021/jp100938v.
- [15] Holló, A.; Hancsok, J.; Kalló, D., Kinetics of hydroisomerization of C5-C7 alkanes and their mixtures over platinum containing mordenite, *Appl. Catal. A: Gen.* **2002**, *229*, 93-102, DOI: 10.1016/S0926-860X(02)00018-2.
- [16] Demirci, Ü. B.; Garin, F., Kinetic study of n-heptane conversion on sulfated zirconia-supported platinum catalyst: The metal-proton adduct is the active site, *J. Mol. Catal. A: Chem.* **2002**, *188*, 233-243, DOI: 10.1016/S1381-1169(02)00337-0.